Fusion Engineering and Design 17 (1991) 131–137
North-Holland

Thermal control of solid breeder blankets

A.R. Raffray, A. Ying, Z. Gorbis, M.S. Tillack and M.A. Abdou

Mechanical, Aerospace and Nuclear Engineering Department, University of California, Los Angeles, CA 90024-1597, USA

An assessment of the thermal control mechanisms applicable to solid breeder blanket designs under ITER-like operating conditions is presented in this paper. Four cases are considered: a helium gap; a sintered block Be region; a sintered block Be region with a metallic felt at the Be-clad interface; and a Be packed bed region. For these cases, typical operating conditions are explored to determine the ranges of wall load which can be accommodated while maintaining the breeder within its allowable operating temperature window. The corresponding region thicknesses are calculated to help identify the praticality of each concept and the design tolerances.

1. Introduction

Thermal control is an important issue for solid breeder blankets since the breeder needs to operate within its temperature window for the tritium release and inventory to be acceptable. For an experimental reactor like ITER, where power production is not an objective, the coolant can be kept at low temperature and low pressure to enhance reliability and safety. In order to maintain the solid breeder above its minimum allowable temperature, a thermal resistance region must then be provided between the solid breeder and coolant, as shown in fig. 1.

The two types of thermal resistance proposed for the ITER base blanket [1] are: a thin He gap; or a Be region which would perform both neutron multiplying and thermal barrier functions. The Be could be either in sintered block or packed bed form. In addition for the case of Be sintered blocks which have a high thermal conductivity, it is conceivable that a felt-like material would be inserted at the Be-clad interface in order to increase the overall thermal resistance of the thermal control region, and, thus, reduce the Be inventory if required.

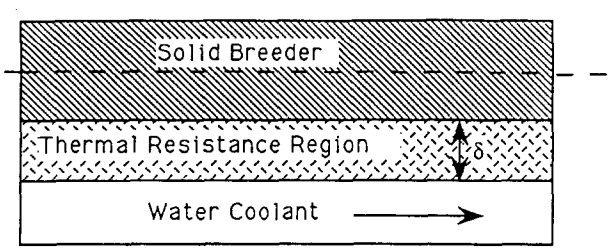

Fig. 1. Scheme of thermal resistance region between high-temperature solid breeder region and low-temperature water coolant.

Thermal control issues involve the predictability and controllability of the thermal resistances particularly during operation. An active control mechanism can alleviate some of these concerns and help accommodate power variation, which is necessary in experimental fusion devices such as ITER. This paper evaluates the proposed thermal control schemes for solid breeder blankets and assesses their potential as both passive and active control mechanisms based on example calculations for ITER-relevant conditions.

2. Helium gap

Use of a He gas as thermal barrier is attractive based on the simplicity of the configuration and the well-known properties of He. It has been used successfully in smallscale in-situ tritium release experiments in fission reactors. However, for ITER-like power densities, the He gap thickness, δ_{He}, required to produce the necessary temperature drop between the coolant and breeder is small (of the order of 1 mm) and the resulting thermal resistance is sensitive to even small changes in the geometry. Thus, for large-scale blanket application, the key concern remains the close tolerance required during manufacture and assembly and the ability to predict the gap dimensions during operation. This concern is exacerbated if the blanket configuration requires a variable δ_{He} to account for spatial

power density variation and bending of the blanket to accommodate space restriction or reactor contours, such as in the case of a poloidal blanket tube geometry.

To illustrate the range of δ_{He} applicable to an ITER blanket using Li_2O as breeder, the range of allowable neutron wall loads was calculated as a function of the helium gap thickness between the solid breeder and water coolant based on the following assumptions:

(1) a Li_2O heat generation of 20 MW/m^3 based on a neutron wall load, P_N, of 1.2 MW/m^2;
(2) a solid breeder layer thickness of 1 cm, which results in a heat flux to the thermal resistance region of 0.1 MW/m^2 and a Li_2O temperature drop of 100 K, respectively;
(3) Li_2O minimum and maximum allowable temperatures, $T_{SB(min)}$ and $T_{SB(max)}$, of 673 K and 1273 K;
(4) a constant water temperature of 343 K;
(5) a coolant film drop, ΔT_f, of 30 K for a P_N of 1.2 MW/m^2; and
(6) negligible temperature drops across the Stainless Steel (SS) clads.

The He thermal conductivity, k_{He}, increases with temperature (shown as part of fig. 6). This is an attractive characteristic since it effectively extends the range of allowable power variation. Typically, as the power is increased, the temperature drop across the He gap increases but because of the enhanced k_{He}, the increase is not in direct proportion to the power increase. This results in maintaining the solid breeder temperature within its allowable window over larger power variation. These effects were included in the calculations. First, the temperature drop across each region was calculated for a P_N of 1.2 MW/m^2 and for the given assumptions. The maximum allowable P_N was then estimated as f_{max}, a multiple of 1.2 MW/m^2, as follows:

$$f_{max}\left[\Delta T_{f(0)} + \left(k_{He(0)}/k_{He(1)}\right)\Delta T_{He(0)} + \Delta T_{SB(0)}\right] = T_{SB(max)} - T_{water}, \quad (1)$$

where the subscripts (0) and (1) refer to parameters calculated for the reference and final P_N values. $k_{He(1)}$ can be estimated from the He average temperature, $T_{He(1)}(av)$, based on the variation of k_{He} with temperature. $T_{He(1)}(av)$ is given by

$$T_{He(1)}(av) = T_{water} + f_{max}\left[0.5\left(k_{He(0)}/k_{He(1)}\right)\Delta T_{He(0)} + \Delta T_{f(0)}\right]. \quad (2)$$

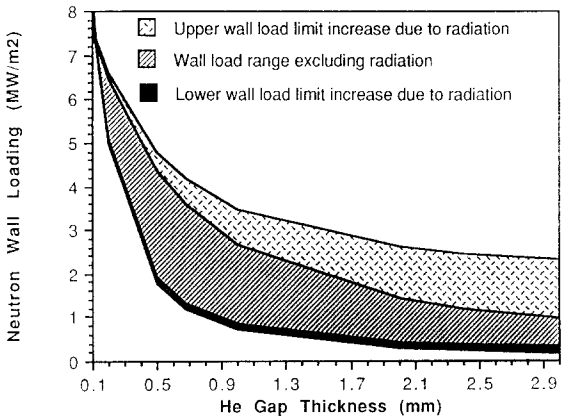

Fig. 2. Range of allowable P_N as a function of δ_{He} including and excluding radiation heat transfer. For the case with radiation, the maximum allowable P_N range is shown based on the assumption of black surfaces.

Equations (1) and (2) in conjunction with the variation of k_{He} with temperature were solved for the three unknowns, $k_{He(1)}$, $T^{(av)}_{He(1)}$, and f_{max}. Equation (1) was replaced by the following expression to calculate the minimum allowable P_N as f_{min}, a multiple of 1.2 MW/m^2:

$$f_{min}\left[\Delta T_{f(0)} + \left(k_{He(0)}/k_{He(1)}\right)\Delta T_{He(0)}\right] = T_{SB(min)} - T_{water}. \quad (3)$$

In addition, radiation can contribute significantly to the heat transfer particularly for the high-temperature cases. Radiation is dependent on the emissivity of the surfaces, which is not known. As an upper bound, the effect of radiation was included based on the Stefan–Boltzmann law for a black surface.

The results are shown in fig. 2 for cases with and without radiation. The allowable P_N range contracts rapidly as δ_{He} is decreased. In the absence of radiation, δ_{He} for a reasonable range of P_N (0.55–2 MW/m^2) is about 1.5 mm, which is small and gives rise to the concern of maintaining close tolerances during manufacture and operation. Radiation substantially increases the allowable upper wall load limit and would allow the choice of a larger gap size, depending on the emissivity of the surfaces. The effect is more marked for cases where the allowable wall load and corresponding heat flux are initially lower since the additional heat flux allowed by radiation for the same temperature drop across the gap is then relatively more important. Similarly, radiation also slightly increases the lower allowable wall load but the effect is

small since the temperatures involved are lower. For example, for a 3 mm gap thickness, the allowable wall range of 0.19–0.96 MW/m^2 excluding radiation is extended to a maximum of 0.32–2.32 MW/m^2 when including radiation. The actual range would be somewhere between these two ranges depending on the emissivity of the surfaces.

The blanket operating flexibility could be increased if a means of active control of the thermal resistance region was provided. For a He gap, two possible means of controlling its conductance are: (1) a change in gas pressure; and (2) a change in the gas flow rate if the helium could be flowed.

The possibility of k_{He} control through pressure adjustment was assessed. Conduction must take place at least in part in the molecular regime for pressure to affect the k_{He}, and, thus, the characteristic conduction distance with respect to the temperature jump distance (based on the gas mean free path) becomes a key factor. k_{He} was calculated for different gap thicknesses and pressures based on the dependence of the temperature jump distance on pressure and assuming an average temperature of 573 K and a conservative thermal accommodation coefficient of 0.4 for He (Ullman [2]). It is believed that for reactor application, the lowest practical operating pressure for He is of the order of 0.1 atm. The ratio of k_{He} at 1 atm to k_{He} at 0.1 atm is used as a measure of active thermal control. The higher pressure of 1 atm is chosen since, even for the smallest δ_{He} considered (0.1 mm), k_{He} tends to saturate at about this pressure. The results are illustrated in fig. 3. Also shown in the figure is the temperature drop across the He gap for the example case considered. It can be seen that while the degree of k_{He} control increases with decreasing δ_{He}, the gap temperature drop decreases. These two effects tend to cancel each other, so that for this case, the allowable power variation provided by active control is always less than 2% even for a 0.1 mm gap.

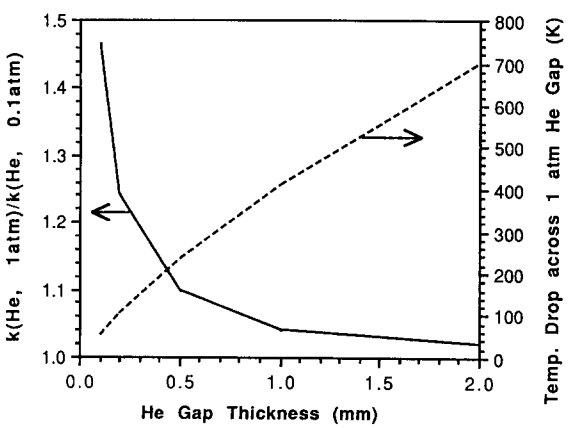

Fig. 3. Ratio of k_{He} at 1 atm to k_{He} at 0.1 atm as a function of δ_{He}. The temperature drop across the He gap is also shown assuming a heat flux of 0.1 MW/m^2.

To assess the possibility of thermal control through flow rate adjustment for flowing helium, the variation of the Nusselt number, Nu, with the Reynolds number. Re, was considered. For fully developed laminar flow, Nu depends on the boundary conditions but not on the flow rate. In the turbulent regime, Nu increases substantially with increasing Re; however, the corresponding pressure drop also increases. For example, for a Re of 10^4, the pressure drop is higher than 2 atm/m for a 2 mm gap and jumps to 17 atm/m for 1 mm gap. The above discussion indicates that significant active control through pressure and/or flow rate variation is not possible for the He gap.

3. Beryllium region

The thermal resistance between the solid breeder and coolant can also be provided by a Be region, which performs the dual function of neutron multiplication and thermal control. Use of Be sintered blocks offer the advantage of relatively thick regions, which results in minimizing the number of solid breeder and Be layers. However, it also results in the use of large amount of Be whose resources are limited and whose unit cost is high. In addition, the tritium breeding benefit gained from using Be as a neutron multiplier tends to saturate with a Be thickness within about 10–12 cm, depending on the blanket configuration (Abdou [3]). Two possible ways of minimizing the use of Be in he blanket are to insert a metallic felt at the Be sintered block–clad interfaces or to use a packed bed of Be, at least for the thicker Be block regions. Both of these configurations would also provide the possibility of active thermal control, which is not available in the pure Be sintered block case.

The three configurations: Be sintered block, Be sintered block with metallic felt, and Be packed bed are discussed in the following sub-sections.

3.1. Be sintered block

Beryllium in sintered block form has a high thermal conductivity, k_{Be}, and depending on the heat generation in the solid breeder and Be, the Be region thick-

ness, δ_{Be}, can be quite high in order to provide the required temperature drop between the solid breeder and coolant. For a multi-layer solid breeder blanket under ITER conditions, such as that of ref. [4], δ_{Be} varies from about 3–15 cm depending on the radial and poloidal position of the blanket segment. Concerns with the sintered block configuration have been covered in previous publications ([4] and Billone [5]). They arise mainly because of the large value of k_{Be}/k_{He} (of the order of 400) which results in even small He gap formation having a significant effect on the temperature drop across the thermal resistance region. Of particular concern are the Be block deflection under thermal expansion and the predictability of the Be–clad interface thermal resistance during operation, which was addressed in ref. Gorbis [6] based on the models of refs. Lemczyk [7] and Shlykov [8].

The range of allowable P_N based on the allowable temperature window of the solid breeder was calculated for the Be sintered block case based on the same assumptions as listed in the previous section for the He gap case. In addition, the contact conductance at the Be–clad interfaces was assumed to be 2000 W/m^2 K and the heat generation in the Be was set at 3 MW/m^3 for a P_N of 1.2 MW/m^2. As opposed to k_{He}, k_{Be} decrease with increasing temperature (also shown as part of fig. 6), which limits the allowable P_N range. This was taken into account in the calculations. Equations similar to eqs. (1), (2) and (3) but with additional terms for temperature drops at the two Be–clad interfaces were used in conjunction with the variation of k_{Be} with temperature in order to calculate f_{min} and f_{max}. The results shown in fig. 4. It should be noted that any uncertainty in the parameters affecting the solid breeder temperature would effectively reduce the allowable wall load range shown in the figure. For operating at P_N of 1.2 MW/m^2, δ_{Be} should be between 4.2 and 8.6 cm. A δ_{Be} of about 5.3 cm would enable accomodation of a reasonable P_N range of 1–2 MW/m^2.

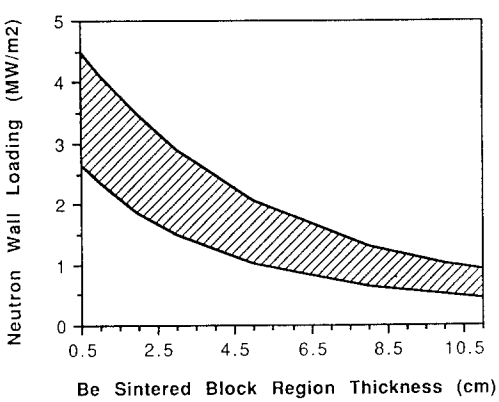

Fig. 4. Range of allowable P_N as a function δ_{Be}.

3.2. Be sintered block with metallic felt

Placing a metallic felt at the breeder interface has been proposed in ref. [9] to provide a reasonable degree of contact resistance predictability. Additionally, a metallic felt at the Be–clad interface would provide advantages of accommodation of Be swelling and thermal expansion through felt compressibility and the possibility of active thermal control through gas pressure adjustment. Issues relate to the performance of the felt material in an irradiation environment, which would need to be addressed experimentally, and to the effect of additional steel on the tritium breeding.

Manufactured metallic felt are available with theoretical densities ranging from at least 10–60%, and with fibers as small as 8 μm. The effect of gas pressure on the felt thermal conductivity, k_{felt}, was estimated by applying the model of Kunii [10] for porous material to the felt case. A simple rectangular configuration was assumed for the felt fibers and the gas characteristic distance was estimated as a function of the porosity for an assumed fiber diameter of 8 μm, and used in order to calculate the interstitial gas conductivity as a function of pressure in the model. For SS-316 felt and He, the results indicate a ratio of k_{felt} at 1 atm to k_{felt} at 0.1 atm of about 1.6 for a felt porosity of 15% and of about 1.7 for a felt porosity of 40%, with associated k_{felt} values at 1 atm of about 2.7 W/m K and 1.3 W/m K respectively for each case.

For the example calculations, a SS-316 felt was assumed to be located at the low-temperature Be–clad interface, and the other assumptions used in the previous calculations were maintained for consistency. The Be thickness was adjusted based on δ_{felt} so as to keep the same overall temperature drop across the thermal resistance region as for the chosen reference case, where δ_{Be} without the felt is 5.3 cm (see fig. 4). The reduction in the total heat generation in the Be region as its thickness decreases was taken into account. The controllability was calculated from the ratio of k_{felt} at 1 atm to k_{felt} at 0.1 atm (1.7) and was used to estimate the lower limit of allowable P_N while the maximum allowable P_N is kept at 2 MW/m^2. The f_{min} calculation proceeded in a manner similar to that of the pure sintered block case except that the felt temperature drop was increased by a k_{felt} controlability factor of 1.7 to account for active control.

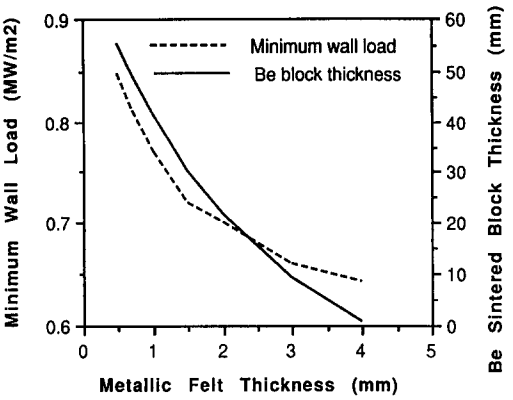

Fig. 5. Minimum allowable wall load as a function of δ_{felt} for the case where δ_{Be} without the felt is 5.3 cm (see fig. 4) and the maximum allowable P_N is kept at 2 MW/m^2. The additional Be sintered block thickness to provide the required thermal resistance is also shown.

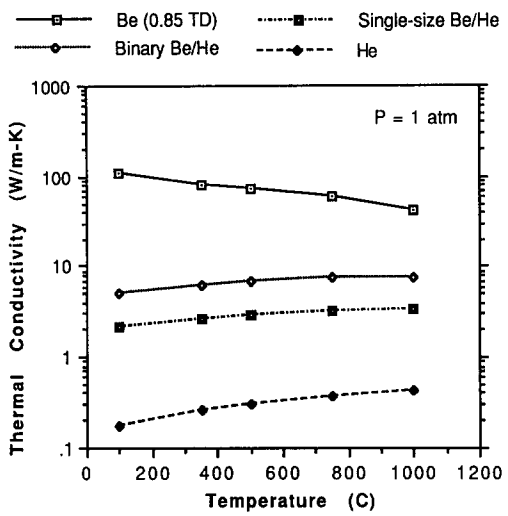

Fig. 6. Thermal conductivity of Be, He and single-size (1 mm, $\epsilon = 0.37$) and binary (1.3+0.2 mm, $\epsilon = 0.18$) packed beds of Be–He (neglecting radiation) as a function of temperature.

Figure 5 shows the active control provided by the felt as a function of the felt thickness. Also shown is the corresponding Be block thickness. The effect of including a felt at the Be-clad interface can be seen to provide significant active control, lowering the allowable P_N from 1 MW/m^2 for the case without the felt to about 0.7 MW/m^2 for a case with a δ_{felt} of 2 mm. The corresponding Be thickness is 2.2 cm, a substantial reduction from the original 5.3 cm value without the felt.

3.3. Be packed bed

The packed bed form offers advantages of active control of the thermal conductance of the Be region through adjustment of the gas pressure or composition and minimum use of Be since the lower thermal conductivity of the packed bed results in thinner Be layers as compared to the sintered block form. However, this may lead to a larger number of layers, and, thus, to a more complex design, as dictated by the neutronics for optimum tritium breeding.

Figure 6 shows the effective thermal conductivity, k_{eff}, of a single-size and binary Be–He packed beds at 1 atm as a function of temperature based on calculations from the model described in Adnani [11]. As mentioned before, also shown are the helium and Be thermal conductivities. As noted earlier, k_{Be} decreases with temperature while k_{He} increases, the resulting effect being a slight increase in k_{eff} with temperature for both packed beds, which was incorporated in the example calculation described below. Recent data and modeling analyses (Adnani [11], Tillack [12]) have confirmed the sharp effect of gas pressure and composition changes on k_{eff} of Be–He packed beds. In fact, as indicated in fig. 7, for a single-size packed bed case, the pressure controllability (expressed as the ratio of k_{eff} at 2 atm to k_{eff} at 0.2 atm) peaks at a solid to gas conductivity ratio of about 400–500, which corresponds exactly to the Be to He conductivity ratio. Gas composition change (e.g. from He to Ne) also changes k_{eff} appreciably. However, because of the possible com-

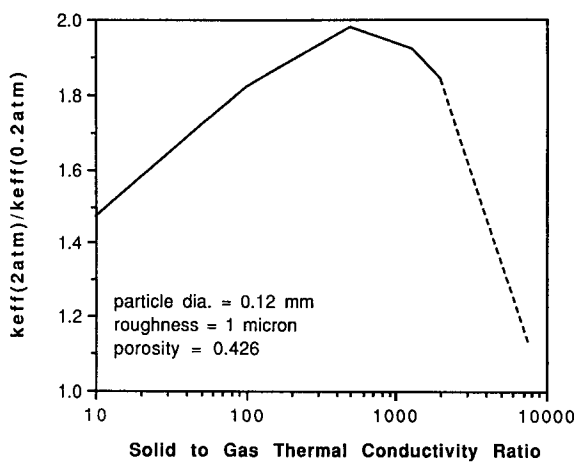

Fig. 7. Pressure control of single-size packed bed k_{eff} as a function of solid to gas conductivity ratio.

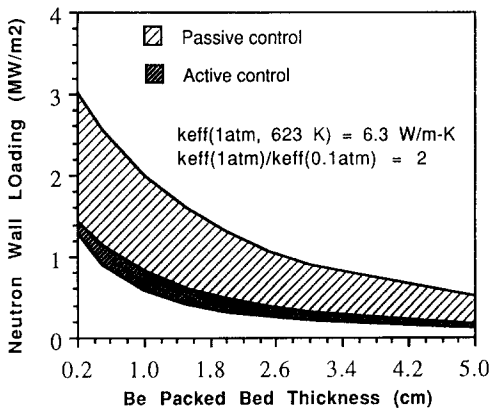

Fig. 8. Range of allowable P_N based on the solid breeder temperature limits as a function of δ_{bed}.

plexities involving the use of two gases, it is not considered here.

An example calculation similar to the previous ones was done for the Be packed bed assuming a binary bed and a ratio of k_{eff} (1 atm)/k_{eff}(0.1 atm) of 2 (estimated from Adnani [11]) and applying the same assumptions as before. The only exception is the packed bed wall conductance which was conservatively set at 1000 W/m^2 K, in the belief that it should be lower than the sintered block–clad contact conductance. The final k_{eff} value was estimated from the corresponding average bed temperature based on the variance of the binary bed k_{eff} with temperature shown in fig. 6. The active control was calculated by increasing the temperature drop across the Be bed by the k_{eff} controllability factor of 2 in the calculation of f_{min}. The results are shown in fig. 8 in terms of the allowable P_N range as a function of the Be packed bed region thickness, δ_{bed}, based on both passive and active thermal control. In this case, for a P_N of 1.2 MW/m^2, δ_{bed} ranges from about 3 mm to 2.2 cm. As compared to fig. 4, the packed bed form seems to offer a wider allowable P_N range, relevant to ITER. For example, for a packed bed thickness of 1 cm, the passive P_N range is about 0.82–2.0 MW/m^2, while active control enables operation at a lower P_N of 0.58 MW/m^2. It must be noted, though, that δ_{bed} is limited by the size of the Be particles. For single-size bed, to minimize wall effect the ratio of δ_{bed} to particle diameter should be at least about 10, while for binary mixture this requirement is somewhat relaxed. It should also be noted that the allowable P_N range would appreciably increase if the the wall conductance is higher than the assumed value of 1000 W/m^2 K. The effect of radiation on the Be–He packed bed heat transfer was also assessed based on the model of Hall [13] and was found to only slightly increase the allowable wall load range.

4. Summary

An assessment of the thermal control mechanisms applicable to solid breeder blanket designs under ITER-like operating conditions was performed. Four cases were considered: a helium gap; a sintered block Be region; a sintered block helium region with a metallic felt at the Be–clad interface; and a Be packed bed region. Table 1 summarizes the results for an ITER-relevant example case. It should be noted that the allowable P_N range shown assumes no uncertainties in the prediction of calculation parameters. Any changes in these parameters during operation would shift or reduce the P_N range.

A He gap is attractive based on the simplicity of the design and allows for a large wall load range for the example case considered. Radiation heat transfer can substantially extend the allowable wall load range depending on the emissivity of the surfaces. However, the gap size required is still small, leading to concern of maintaining close tolerances during manufacture and operation. The calculations also indicate that significant active control is not possible for the He gap.

Be in sintered block form has a high thermal conductivity, which results in a thick Be layer. This tends to minimize the number of layers, but can result in large amount of Be whose resources are limited and

Table 1
Allowable wall load range and region thickness for different thermal barrier schemes, based on example case calculations (for the He gap case with radiation, black surfaces are assumed)

Thermal barrier type	Thickness	Range of wall load
He gas	1.5 mm	0.55–2 MW/m^2 without radiation
		0.68–3 MW/m^2 with radiation
	3 mm	0.19–0.96 MW/m^2 without radiation
		0.32–2.32 MW/m^2 with radiation
Be sintered block	5.3 cm	1–2 MW/m^2
Be sintered block + felt	2.2 cm + 0.2 mm	0.7–2 MW/m^2
Be packed bed	1 cm	0.58–2 MW/m^2

whose cost is high. The allowable P_N range tends to be smaller than in the other cases because the decrease of k_{Be} with temperature and of the absence of active control mechanism. A key concern is the predictability of the Be–clad interface thermal resistance during operation.

Placing a felt at the Be-clad interface provides advantage of potentially better contact conductance predictability, accomodation of Be swelling and thermal expansion, and possibility of active thermal control through gas pressure adjustment. For the example considered, a felt thickness of 2 mm at the low temperature Be-clad interface reduces the lower allowable P_N from 1 to 0.7 MW/m^2, and results in much thinner Be block. Issues relate mainly to the performance of the felt in an irradiation environment.

Be in packed bed form offers advantages of active control through gas pressure adjustment and minimum use of Be based on its lower thermal conductivity. However, this might lead to a higher number of layers in the design. For the binary packed bed considered, the ratio of k_{eff} at 1 atm to k_{eff} at 0.1 atm is about 2. This provides substantial additional flexibility for power variation accomodation through active thermal control, resulting in a wider allowable P_N range than for the sintered block cases.

Acknowledgement

This work was performed under U.S. Department of Energy Contract DE-FG03-88ER52150.

Nomenclature

f_{min}, f_{max}	minimum and maximum allowable multiples of the reference neutron wall load, 1.2 MW/m^2,
k_{He}, k_{Be}	thermal conductivity of He and Be, respectively,
k_{eff}	effective thermal conductivity of packed bed,
P_N	neutron wall load at the first wall,
$T_{bed}, T_{He}, T_{water}$	temperature of packed bed, helium, and water coolant, respectively,
$T_{SB(max)}, T_{SB(min)}$	maximum and minimum allowable solid breeder temperature,
ϵ	packed bed porosity,
δ	thickness of thermal resistance region between solid breeder and coolant,
$\delta_{He}, \delta_{Be}, \delta_{felt}, \delta_{bed}$	thickness of He, Be sintered block, felt and Be–He packed bed region, respectively,
$\Delta T_{He}, \Delta T_f, \Delta T_{SB}$	He, film, and solid breeder temperature drop, respectively.

References

[1] ITER blanket, shield and materials data base, ITER Documentation Series no. 29, IAEA (1991).
[2] A. Ullman, R. Acharya and D.R. Olander, Thermal accomodation coefficients of inert gases on stainless steel and UO_2, J. Nucl. Mater. 51 (1974) 277–279.
[3] M.A. Abdou, M.S. Tillack, A.R. Raffray, A.H. Hadid, et al., Modeling analysis and experiments for fusion nuclear technology, FNT Priogress Report: Modeling & FINESSE, PPG-1021, UCLA-ENG-86-44, FNT-17, University of California, Los Angeles (January 1987).
[4] U.S. Technical Report for the ITER Blanket/Shield-A. Blanket, ITER-TN-BL-5-0-3, Garching, Germany (July–November 1990).
[5] M.C. Billone, S. Majumbar, H. Hashizume, and A.R. Raffray, Thermal-mechanical analyses of the Be multiplier zones, Report of U.S. Contributions to the Homework for ITER, (February, March 1989).
[6] Z. Gorbis, A.R. Raffray and M.A. Abdou, Study of effective solid-to-solid contact thermal resistance and its application to solid breeder blanket design for ITER, presented at the Ninth Topical Meeting on the Technology of Fusion Energy, Oak Brook, Illinois (October 1990).
[7] T.E. Lemczyk and M.M. Yovanovich, New models and methology for predicting thermal contact resistance, Heat-Transfer Engin., V.8, N2 (1987) pp. 35–48.
[8] Ju.P. Shlykov, E.A. Ganin and S.N. Tsarevsky, Contact thermal resistance, Energia, Moskow (1977) pp. 327 (in Russian).
[9] Blanket Comparison and Selection Study, Argonne National Laboratory, ANL/FPP-83-1, Vol. II (1983).
[10] D. Kunii and J.M. Smith, Heat transfer characteristics of porous rock, A.I.Ch. J. 6 (1960) 71–78.
[11] P. Adnani, Modeling of effective thermal conductivity for a packed bed, Ph.D. Dissertation, University of California, Los Angeles (1991).
[12] M.S. Tillack, A.R. Raffray, A.Y. Ying, P. Huemes and M.A. Abdou, Experimental studies of active temperature control in solid breeder blankets, ISFNT-2, Karlsruhe, 2–7 June 1991, Fusion Engrg-Des. 17 (1991) 165–170, in these Proceeding, Part B.
[13] R.O.A. Hall and D.G. Martin, The thermal conductivity of powder beds. A model, some measurements on UO_2 vibro-compacted microspheres, and their correlation, J. Nucl. Mater. 101 (1981) 172–183.